

Lighting up alkaline phosphatase in the Drug-induced liver injury using a new chemiluminescence resonance energy transfer nanoprobe

Xueting Liu,‡ Nannan Fan,‡ Lijie Wu, Chuanchen Wu, Yongqing Zhou, Ping Li,* and Bo Tang *

College of Chemistry, Chemical Engineering and Materials Science, Institute of Biomedical Sciences, Collaborative Innovation Center of Functionalized Probes for Chemical Imaging in Universities of Shandong, Key Laboratory of Molecular and Nano Probes, Ministry of Education of Molecular and Nano Science, Shandong Normal University, Jinan 250014, PR China

E-mail: tangb@sdu.edu.cn; lip@sdu.edu.cn

Table of Contents

Materials and Instruments

Synthetic procedures of MSN@RhB@ β -CD@AMPPD

The effect on CL by changing the MSN@RhB@ β -CD/AMPPD ratios

Determination the capacity of RhB in MSN@RhB@ β -CD@AMPPD

Measurement of RhB leakage from MSN@RhB@ β -CD@AMPPD

Measuring the amount of AMPPD assembled in MSN@RhB@ β -CD@AMPPD

Cells/mice culture

Table S1 The size distribution of MSN@RhB@ β -CD@AMPPD by DLS

Table S2 Comparison of various fluorescent methods for detecting ALP

Figure S1 The effect on CL by changing the MSN@RhB@ β -CD/AMPPD ratios

Figure S2 The N₂ adsorption-desorption isotherms of MSN

Figure S3 Standard linear calibration curve of RhB

Figure S4 Release curve of RhB from MSN@RhB@ β -CD@AMPPD over time

Figure S5 Standard linear calibration curve of AMPPD

Figure S6 CL time of MSN@RhB@ β -CD@AMPPD to ALP

Figure S7 The photostability of MSN@RhB@ β -CD@AMPPD

Figure S8 CL responses of MSN@RhB@ β -CD@AMPPD toward other biorelevant substances

Figure S9 CL intensities of MSN@RhB@ β -CD@AMPPD with or without inhibitor

Figure S10 The MTT assay of HL-7702 cells with MSN@RhB@ β -CD@AMPPD

Figure S11 The effect of MSN@RhB@ β -CD@AMPPD concentration on CL signals to ALP

Figure S12 The CL imaging of MSN@RhB@ β -CD@AMPPD in Hela cells

Figure S13 The CL imaging of MSN@RhB@ β -CD@AMPPD in HepG2 cells

Figure S14 The hematoxylin and eosin (H&E) staining of liver

Materials and Instruments

Tetraethyl orthosilicate (TEOS), hydrochloric acid (HCl), N, N-Dimethylformamide (DMF), and ethanol were purchased from Shanghai Reagent Co. Ltd. (Shanghai, China). 3-Aminopropyltriethoxysilane (APTES) and rhodamine B (RhB) were purchased from Tianjin Heowns Biochemical Technology Co., Ltd. (Tianjin, China). Alkaline Phosphatase (ALP), β -Cyclodextrin (β -CD), 3-[2-spiroadamantane]-4-methoxy-4-[3-phosphoryloxy]-phenyl-1,2-dioxetane Dioxetane (AMPPD), 3-(4,5-dimethylthiazol-2-yl)-2,5-diphenyltetrazolium bromide (MTT) were purchased from Sigma-Aldrich (St. Louis, U.S.A.). Levamisol hydrochloride was purchased from Macklin (Shanghai, China). α -Naphthyl isothiocyanate (ANIT) was purchased from Aladdin (Shanghai, China). The human cervical carcinoma HeLa cells, hepatocyte line HL-7702 and human hepatoma cells HepG2 were purchased from Cell Bank of the Chinese Academy of Sciences (Shanghai, China). KM mice were purchased from the Animal Living Center of Shandong University. The water used in experiments was all Mill-Q doubly distilled water ($18.2 \text{ M}\Omega \cdot \text{cm}^{-1}$). All reagents were purchased commercially and used without further purification.

The mass spectra were obtained by Bruker maXis ultra-high resolution-TOF MS system. The fluorescence spectra were recorded on FLS-920 Edinburgh fluorescence spectrometer. Transmission electron microscopy (TEM) was carried out on a HT7700 electron microscope. Absorption spectra were measured on a TU-1900 UV-vis spectrophotometer (Beijing Purkinje General Instrument Co., Ltd.). Absorbance was measured in a microplate reader (RT 6000, Rayto, USA) in the MTT assay. Measurements of Dynamic light scattering (DLS) and zeta-potential were performed on a Malvern zeta sizer Nano-ZS90. CL imaging was acquired by IVIS Lumina II *in vivo* imaging system.

Synthetic procedures of MSN@RhB@ β -CD@AMPPD

Mesoporous silica (MSN) was prepared by a previously reported method.¹ Mono-6-deoxy-6-(p-tolylsulfonyl)-beta-cyclodextrin (6-OTs- β -CD) was obtained according to the literature.² HRMS [M+Na⁺] 1311.3684, found 1311.3613.

MSN@RhB-NH₂: MSN (5.0 mg) was dispersed in 5 mL of anhydrous ethanol, then RhB (5.0 mg) was added to the solution and stirred at room temperature. After 24 h, 5 mL of anhydrous ethanol and 200 μ L of ammonia were added and stirred for another 15 min. Then, 16 μ L of (3-propylamino) triethoxysilane (APTES) was added dropwise to the reaction mixture and kept at 25 °C for 12 h. MSN@RhB-NH₂ nanoparticles were centrifuged and repeatedly washed with anhydrous ethanol.

MSN@RhB@ β -CD: The prepared MSN@RhB-NH₂ (2.0 mg) and 6-OTs- β -CD (17.0 mg) were dispersed in 5 mL ethanol, then the mixture was transferred into flask and stirred for 24 h at 45 °C under Ar gas atmosphere. Thereafter, the nanoconjugates were collected by high-speed centrifugation, and the precipitate was washed with DMF three times for the removal of unreacted 6-OTs- β -CD.

MSN@RhB@ β -CD@AMPPD: MSN@RhB@ β -CD (2.0 mg) was dispersed in 200 μ L of DMF, to which AMPPD (6.5 mg) was added. Under ultrasonic condition, 3 mL of doubly distilled water was dropped to the solution. Then, the ultrasound was kept for 45 min for the acquisition of the final nanoprobe MSN@RhB@ β -CD@AMPPD.

The effect on CL by changing the MSN@RhB@ β -CD/AMPPD ratios

Different doses of AMPPD (1.6, 3.2, 6.5, 13.0, 26.0 mg) were separately added to five EP tubes in which MSN@RhB@ β -CD (2.0 mg) was dispersed with 200 μ L of DMF. Under ultrasonic condition, 3 mL of doubly distilled water was dropped to the solution. Then, the ultrasound was kept for 45 min to obtain five different nanoparticles. At last, each nanoparticle solution with the same concentration was prepared, and CL signals of them were acquired in the presence of ALP. As Figure S1 shown, the CL ratios were remarkably increased and reached around 25.99 at a dose of 6.5 mg AMPPD. Then the CL ratios had no noticeable change with the increase of

AMPPD level. So, we choose 6.5 mg AMPPD to assemble MSN@RhB@ β -CD@AMPPD.

Determination of RhB-loaded in MSN@RhB@ β -CD@AMPPD

Ethanol solutions of RhB with different concentrations (0.01, 0.02, 0.04, 0.06, 0.07, 0.08, 0.09×10^{-3} mg/mL) were prepared. Fluorescence intensity was measured, and the standard curve was drawn. We dispersed MSN@RhB@ β -CD@AMPPD (1.0 mg) in 1 mL of anhydrous ethanol to obtain a concentration of 1.0 mg/mL, and the solution was heated to 75 °C for 2 h until the RhB loaded in the probe was released completely. Then, the fluorescence intensity of the supernatant was measured after high-speed centrifugation. The RhB concentration was determined according to the standard curve, and the amount of RhB-loaded in the MSN@RhB@ β -CD@AMPPD was 0.078 μ g/mg.

Measurement of RhB leakage from MSN@RhB@ β -CD@AMPPD

MSN@RhB@ β -CD@AMPPD (1.0 mg) was dispersed in 1 mL PBS, then the solution was dialyzed in 150 mL doubly distilled water. The fluorescence intensity of the secondary water was measured every 1 hour.

Measuring the amount of AMPPD assembled in MSN@RhB@ β -CD@AMPPD

Water solutions of AMPPD with different concentrations (0.001, 0.01, 0.04, 0.06, 0.08, 0.10×10^{-3} mg/mL) were prepared. Absorbance intensity was measured, and the standard curve was drawn. At the last step of MSN@RhB@ β -CD@AMPPD assembled, all the supernatant was collected after high-speed centrifugation and the absorbance intensity was measured. According to the standard curve, the amount of AMPPD in the MSN@RhB@ β -CD@AMPPD was calculated as 0.075 mg/mg.

Cells/mice culture

Cells were cultured in DMEM with 10% fetal bovine serum and 100 U/mL 1% antibiotics penicillin/streptomycin and maintained at 37 °C in a 100% humidified atmosphere containing 5% CO₂.

In the MTT Assay, HL-7702 cells were seeded at a density of 10⁶ cells/well in a 96-well plate and incubated at 37 °C in a 5% CO₂/95% air for 24 h before the MSN@RhB@β-CD@AMPPD was added. The HL-7702 cells were incubated with 0.05, 0.10, 0.20, 0.50, or 1.00 mg/mL MSN@RhB@β-CD@AMPPD for 24 h. The culture medium was removed, and MTT solution (0.5 mg/mL) was added to each well. After 4 h, the remaining MTT solution was removed, and DMSO (100 μL) was added to each well for the dissolution of the formazan crystals. Absorbance was measured at 490 nm in a microplate reader.

For cells imaging, cells were seeded in a 96-well plate and incubated at 37 °C in a 5% CO₂/95% air. After 12 h, inhibitor (5.0 mM) was added in the right well for 10 min. Then the middle and right wells were treated with 0.50 mg/mL MSN@RhB@β-CD@AMPPD for another 30 min, and the CL images were acquired immediately by an IVIS Lumina II *in vivo* imaging system with open filter (570 ± 10 nm).

KM mice of 8–10 weeks were purchased from The Animal Living Center of Shandong University. ANIT was dissolved in vegetable oil before use. The mice were treated by intragastric administration at a dose of 80 mg/kg. The mice were treated continuously for 3 days and subjected to fasting for solids and liquids for 12 h. After the third day of intragastric administration, the mice were subcutaneously injected with MSN@RhB@β-CD@AMPPD for imaging by IVIS Lumina II *in vivo* imaging system.

Table S1. The size distribution of MSN@RhB@β-CD@AMPPD nanoparticles by DLS.

Size/nm	Mean Number Percent	Size/nm	Mean Number Percent
50.57	4.7	164.2	1.8

58.77	17.3	190.1	1.2
68.06	26.1	220.2	0.8
78.82	21.6	255.0	0.6
91.28	12.3	295.3	0.4
105.7	6.3	342.0	0.3
122.4	3.7	396.1	0.2
141.8	2.5	458.7	0.1

Table S2. Comparison of various fluorescent methods for detecting ALP.

Name	$\lambda_{\text{ex}} / \text{nm}$	$\lambda_{\text{em}} / \text{nm}$	LOD/ U·L ⁻¹	References
HTPQA	410	550	1.36	Angew. Chem. Int. Ed., 2017, 56 , 11788
CyP	690	738	3.00	Anal. Chem., 2017, 89 , 6854
HCAP	430	641/539	0.15	ACS Appl. Mater. Interfaces., 2014, 6 , 17245
coumarin@Tb-GMP	315	450/552	10.00	Anal. Chem., 2015, 87 , 3080
ET-Flu-PO ₄ /TPE	365	514/471	1.50	Biosens. Bioelectron., 2017, 91 , 217
CuNPs	335	565	0.30	Anal. Chem., 2013, 85 , 3797
TPE-phos	312	450	0.20	ACS Appl. Mater. Interfaces., 2013, 5 , 8784

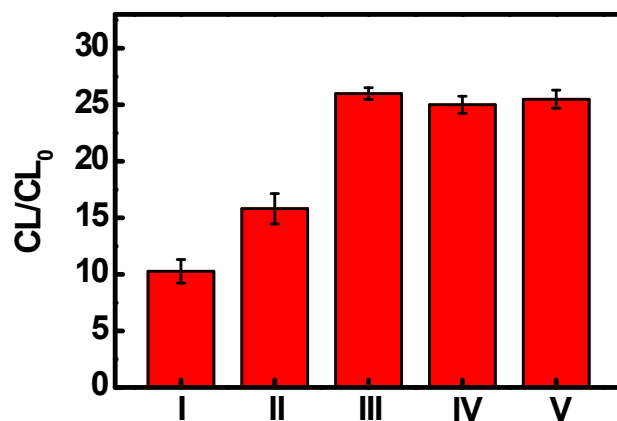


Figure S1. The CL signals of the different ratios of MSN@RhB@ β -CD and AMPPD to ALP. m (MSN@RhB@ β -CD):m (AMPPD) = 2.0:1.6 (I), 2.0:3.2 (II), 2.0:6.5 (III), 2.0:13.0 (IV), 2.0:32.0 (V). ($\lambda_{em} = 570 \pm 10$ nm, Tris-HCl = 50 mM, pH = 9.6, ALP = 200 U/L).

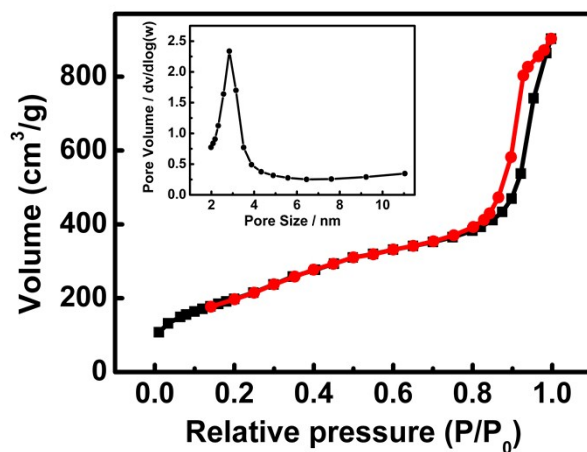


Figure S2. The N₂ adsorption-desorption isotherms of MSN. Insert: pore-size distribution of MSN.

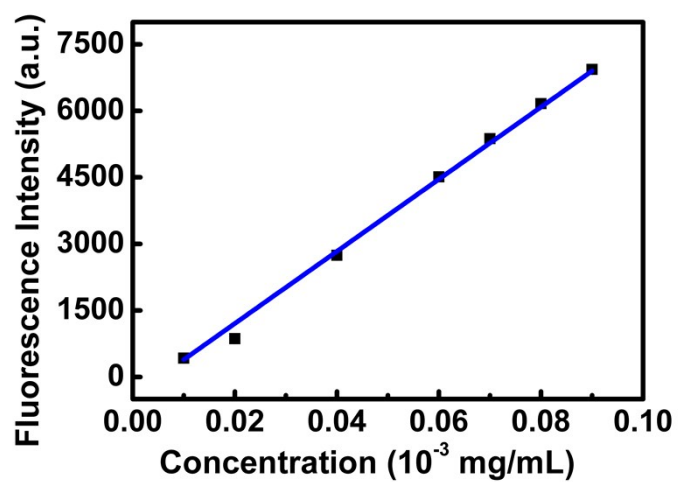


Figure S3. Standard linear calibration curve of RhB.

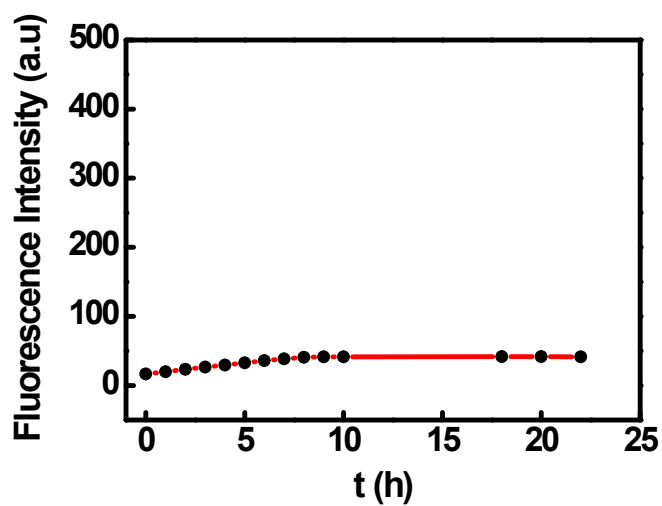


Figure S4. Release curve of RhB from MSN@RhB@β-CD@AMPPD over time, and fluorescence intensities of RhB were almost no change in water.

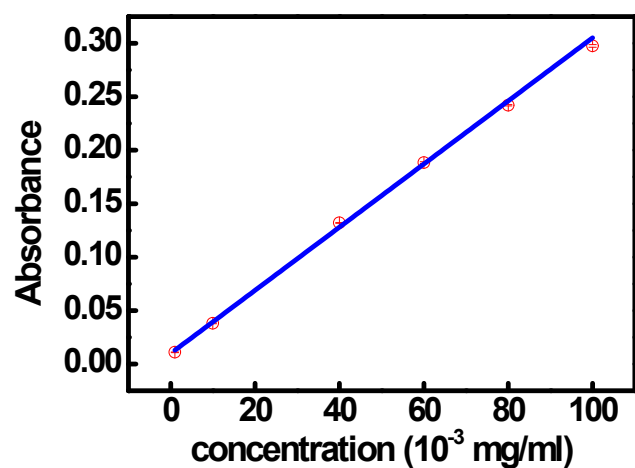


Figure S5. Standard linear calibration curve of AMPPD.

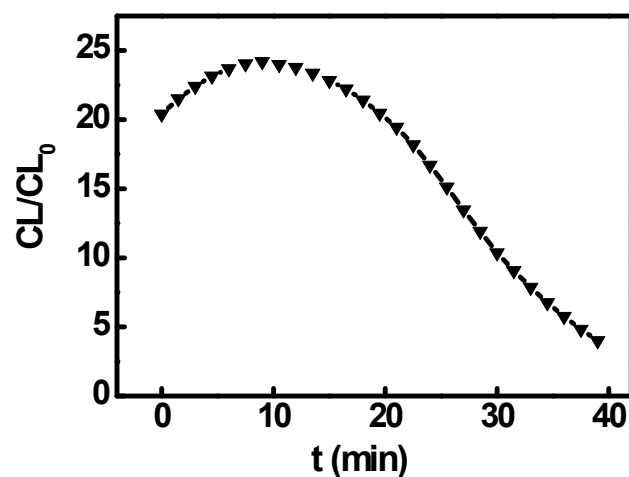


Figure S6. CL changes of MSN@RhB@β-CD@AMPPD ($\lambda_{em} = 570 \pm 10$ nm) in the presence of ALP along time (the probe = 0.50 mg/mL, ALP = 200 U/L, Tris-HCl = 50 mM, pH = 9.6). (CL/CL₀, in which CL and CL₀ represent the emission CL intensity in the presence and the absence of ALP).

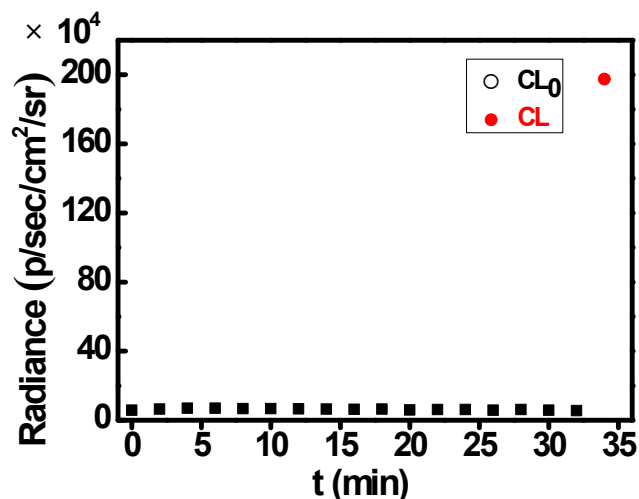


Figure S7. CL intensities (black dots) of MSN@RhB@ β -CD@AMPPD (0.50 mg/mL) in the absence of ALP within 33 min, and the signals remained unchanged. While the CL intensity (red dot) was increased when ALP (200 U/L) added at 34 min.

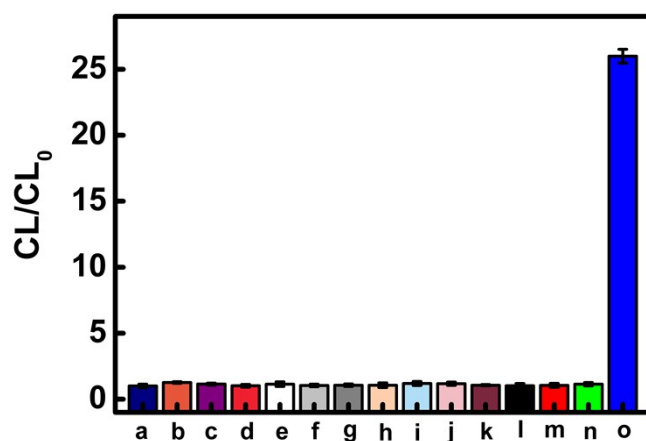


Figure S8. CL responses of MSN@RhB@ β -CD@AMPPD (0.50 mg/ml) toward other biorelevant substances (1.0 mM for b-g, 0.5 mM for h-i, 0.2 mM for j-l, 1.0 mM for ClO^- , 5.0 mM for H_2O_2 , 200 U/L for ALP): (a) blank, (b) L-glutamate, (c) L-tyrosine, (d) L-Cysteine, (e) L-Histidine, (f) GSH, (g) glucose, (h) Ca^{2+} , (i) Mg^{2+} , (j) Zn^{2+} , (k) Fe^{2+} , (l) Fe^{3+} , (m) ClO^- , (n) H_2O_2 , (o) ALP. (CL/CL_0 , in which CL and CL_0 represent the emission CL intensity in the presence and the absence of substances). (Tris-HCl = 50 mM, pH = 7.4 for a-n and pH = 9.6 for ALP).

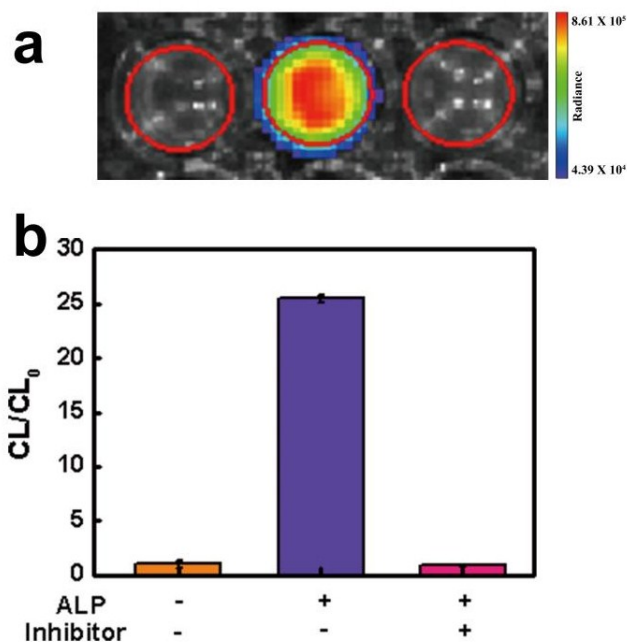


Figure S9. (a) CL intensity of blank (left), ALP (middle), ALP with inhibitor (right). (b) The corresponding CL signals. (the nanoprobe = 0.50 mg/mL, inhibitor = 5.0 mM, Tris-HCl = 50 mM, pH = 9.6, λ_{em} = 570 ± 10 nm).

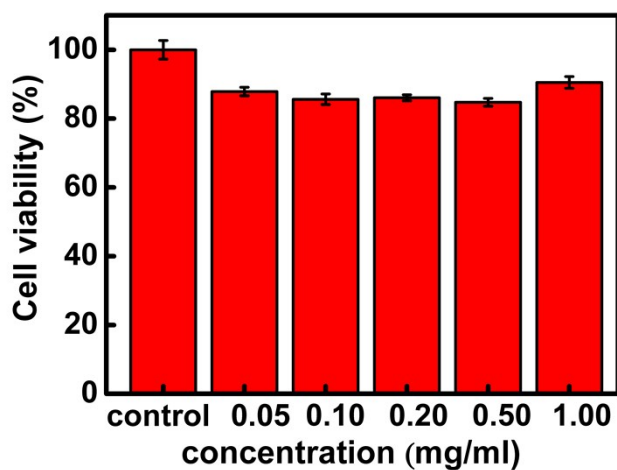


Figure S10. Viability of HL-7702 cells in the presence of different concentrations MSN@RhB@ β -CD@AMPPD, and IC₅₀ was calculated to be 1.03 mg/mL, indicating the low cytotoxicity of MSN@RhB@ β -CD@AMPPD.

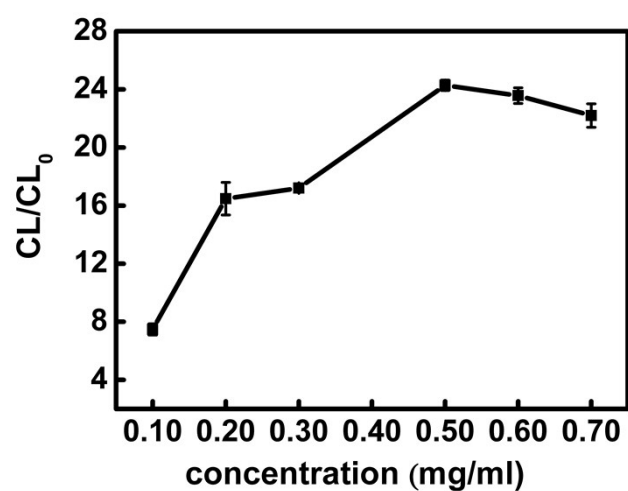


Figure S11. Concentrations of MSN@RhB@β-CD@AMPPD effect on CL signals to ALP (Tris-HCl = 50 mM, pH = 9.6, ALP = 200 U/L).

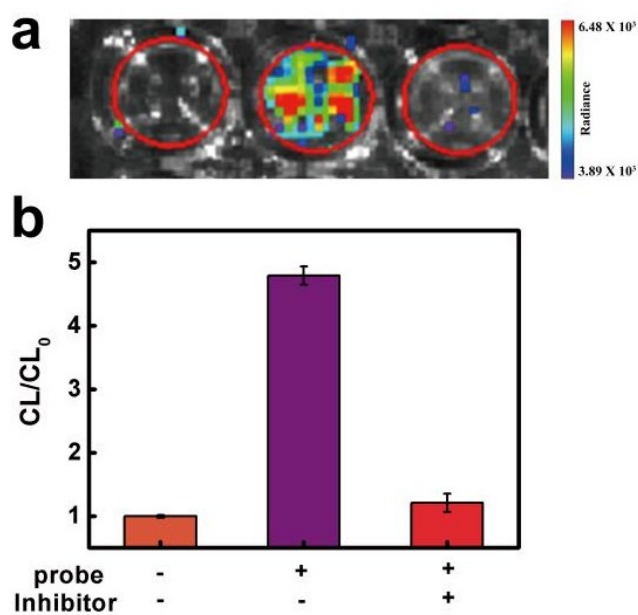


Figure S12. (a) CL images of MSN@RhB@β-CD@AMPPD in HeLa cells by an IVIS Lumina II *in vivo* imaging system with open filter (570 ± 10 nm). Left (first group) was control. Middle (second group) was only treated with 0.50 mg/mL MSN@RhB@β-CD@AMPPD for 30 min. And right (third group) was incubated with 5.0 mM inhibitor, after 10 min, followed by 0.50 mg/mL MSN@RhB@β-CD@AMPPD for 30 min. (b) The corresponding CL intensity quantized output

diagram (CL/CL_0 , in which CL and CL_0 represent the emission CL intensity in the presence and the absence of $MSN@RhB@β\text{-}CD@AMPPD$).

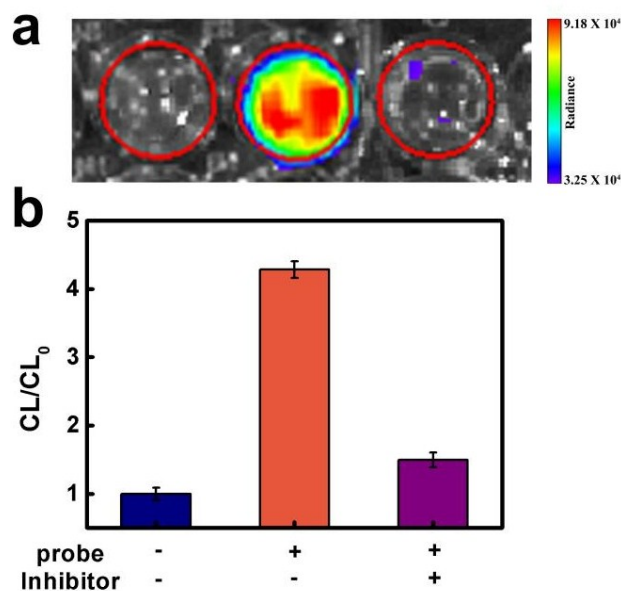


Figure S13. (a) CL images of $MSN@RhB@β\text{-}CD@AMPPD$ in HepG2 cells by an IVIS Lumina II *in vivo* imaging system with open filter (570 ± 10 nm). Left was control. Middle was only treated with 0.50 mg/ml $MSN@RhB@β\text{-}CD@AMPPD$ for 30 min. And right was incubated with 5.0 mM inhibitor, after 10 min, followed by 0.50 mg/ml $MSN@RhB@β\text{-}CD@AMPPD$ for 30 min. (b) The corresponding CL changes. (CL/CL_0 , in which CL and CL_0 represent the emission CL intensity in the presence and the absence of $MSN@RhB@β\text{-}CD@AMPPD$).

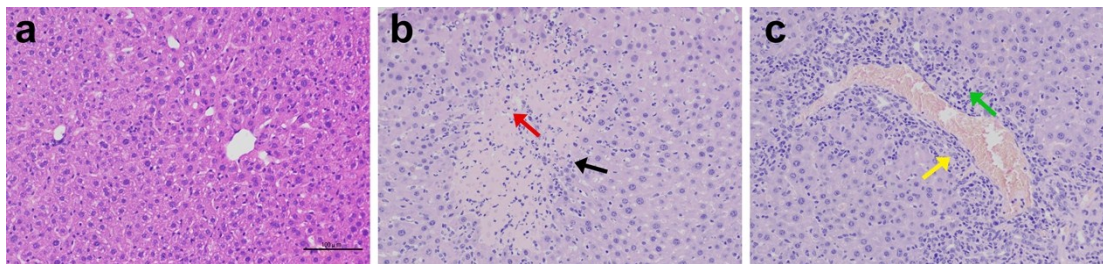


Figure S14. H&E staining. (a) Normal liver tissue. The morphology of hepatocytes is normal, displayed no distinct changes in histological analysis. (b)(c) liver tissue of DILI. Focal necrosis of local hepatocytes, nuclear pyknosis or fragmentation of necrotic hepatocytes (black arrow), neutrophil infiltration (red arrow), proliferation of connective tissue around vein (yellow arrow), accompanied by multiple inflammatory cell infiltration (green arrow). Scale bar = 100 μm .

References

- (1) L. M. Yang, N. Li, W. Pan, Z. Z. Yu, B. Tang, *Anal. Chem.*, 2015, **87**, 3678.
- (2) N. N. Wang, X. Y. Yu, K. Zhang, C. A. Mirkin, J. S. Li, *J. Am. Chem. Soc.*, 2017, **139**, 12354.